Inorg. Chem. **2003**, *42*, 8823–8830

Mono-, Di-, and Tetranuclear Ruthenium(II) Complexes Containing 3-(Pyridin-2-yl)-*as*-triazino[5,6-f]1,10-phenanthroline: Synthesis, Characterization, and Electrochemical and Photophysical Properties

Hui Chao,*,†,‡ Zhi-Ren Qiu,†,§ Li-Rong Cai,‡ Hao Zhang,‡ Xiao-Yuan Li,*,‡ Kam-Sing Wong,§ and Liang-Nian Ji*,†

State Key Laboratory of Optoelectronic Materials and Technologies/Department of Chemistry, Zhongshan University, Guangzhou 510275, P. R. China, and Departments of Chemistry and Physics, Hong Kong University of Science and Technology, Kowloon, Hong Kong, P. R. China

Received July 6, 2003

Mono-, di-, and tetranuclear Ru(II) polypyridine complexes based on the bridging ligand pdtp, where pdtp is 3-(pyridin-2-yl)-as-triazino[5,6-f]1,10-phenanthroline, have been synthesized and characterizated. This asymmetric bridging ligand is composed of two nonequivalent coordinating sites: one involves the phenanthroline moiety, and the other one involves the pyridyltriazine moiety. Electrochemical data show that the first redox process in these complexes is pdtp based and the metal–metal interaction in di- and tetranuclear complexes is very weak. The two oxidations (+1.41 and +1.56 V vs SCE) observed in dinuclear complex **2** are mainly ascribed to the different coordination environments of two metal centers. Absorption spectra are essentially the sum of the spectra of the component monometallic species. The emission spectra are measured both at room temperature and at 80 K in a 4:1 (v/v) EtOH/MeOH matrix. The complexes all display luminescence properties which are close to that featured by the parent $[Ru(phen)_3]^{2+}$ species. It is also noted that center-to-periphery energy transfer occurs in the dendritic tetranuclear complex **3**.

Introduction

Tremendous interest has been attracted to dinuclear and polynuclear Ru(II) polypyridine complexes with regard to the photochemical molecular devices for energy conversion and photoinduced electron (or energy) transfer.[1−15] In most cases, the redox activities and the ground and excited state properties of such complexes are critically dependent on the size, shape, and electronic nature of the bridging ligand. Thus, the design of the bridging ligand is one of the key steps in realizing molecular devices based on polynuclear Ru(II) complexes. Over the past decade, a wide variety of bridging ligands has been introduced to assemble Ru(II) polypyridine building blocks.[1d,1e] However, the vast majority of such studies have been focused on the system containing

* To whom correspondence should be addressed. E-mail: ceschh@zsu.edu.cn (H.C.); chxyli@ust.hk (X.-Y.L.); cesjln@zsu.edu.cn (L.-N.J.). Fax: +86-20-8403 5497 (H.C.).

† Zhongshan University.

‡ Department of Chemistry, HKUST.

§ Department of Physics, HKUST.

(1) (a) Bazani, V.; Scandola, F. *Supramolecular Photochemistry*; Ellis Horwood: Chichester, U.K., 1991. (b) Fabbrizzi, L.; Poggi, A. *Transition Metals in Supramolecular Chemistry*; Kluwer: Dordrecht, The Netherlands, 1994. (c) Balzani, V.; Juris, A.; Venturi, M.; Campagna, S.; Serroni, S. *Chem. Rev.* **1996**, *96*, 759 and references therein. (d) De Cola, L.; Belser, P. *Coord. Chem. Rev.* **1998**, *177*, 301 and references therein. (e) Barigelletti, F.; Flamigni, L. *Chem. Soc. Rev.* **2000**, *29*, 1.

(2) (a) Denti, G.; Campagna, S.; Sabatino, L.; Serroni, S.; Ciano, M.; Balzani, V. *Inorg. Chem.* **1990**, *29*, 4750. (b) Denti, G.; Campagna, S.; Serroni, S.; Ciano, M.; Balzani, V. *J. Am. Chem. Soc.* **1992**, *114*, 2944. (c) Serroni, S.; Juris, A.; Campagna, S.; Venturi, M.; Denti, G.; Balzani, V. *J. Am. Chem. Soc.* **1994**, *116*, 9086. (d) Serroni, S.; Juris, A.; Venturi, M.; Campagna, S.; Resino, I. R.; Denti, G.; Credi, A.; Balzani, V. *J. Mater. Chem.* **1997**, *7*, 1227. (e) Venturi, M.; Serroni, S.; Juris, A.; Campagna, S.; Balzani, V. *Top. Curr. Chem.* **1998**, *197*, 193.

(3) (a) Bolger, J.; Gourdon, A.; Ishow, E.; Launay, J.-P. *Inorg. Chem.* **1996**, *35*, 2937. (b) Ishow, E.; Gourdon, A.; Launay, J.-P.; Lecante, P.; Verelst, M.; Chiorboli, C.; Scandola, F.; Bignozzi, C. A. *Inorg. Chem.* **1998**, *37*, 3603. (c) Ishow, E.; Gourdon, A.; Launay, J.-P.; Chiorboli, C.; Scandola, F. *Inorg. Chem.* **1999**, *38*, 1504.

(4) (a) Lincoln, P.; Norden, B. *Chem. Commun.* **1996**, 2145. (b) Billakhiya, A. K.; Tyagi, B.; Paul, P. *Inorg. Chem.* **2002**, *41*, 3830. (c) Staffilani, M.; Belser, P.; De Cola, L.; Hartl, F. *Eur. J. Inorg. Chem.* **2002**, 335. (d) Staffilani, M.; Belser, P.; Hartl, F.; Kleverlaan, C. J.; De Cola, L. *J. Phys. Chem. A* **2002**, *106*, 9242.

(5) (a) Bodige, S.; Torres, A. S.; Maloney, D. J.; Tate, D.; Kinsel, G.; Walker, A.; MacDonnell, F. M. *J. Am. Chem. Soc.* **1997**, *119*, 10364. (b) Campagna, S.; Serroni, S.; Bodige, S.; MacDonnell, F. M. *Inorg. Chem.* **1999**, *38*, 692. (c) Kim, M.; Konduri, R.; Ye, H.; MacDonnell, F. M.; Puntoriero, F.; Serroni, S.; Campagna, S.; Holder, T.; Kinsel, G.; Rajeshwar, K. *Inorg. Chem.* **2002**, *41*, 2471.

10.1021/ic034769z CCC: $25.00
Published on Web 11/18/2003

Scheme 1. Synthetic Routes for the Preparation of the Ligands and Complexes[a]

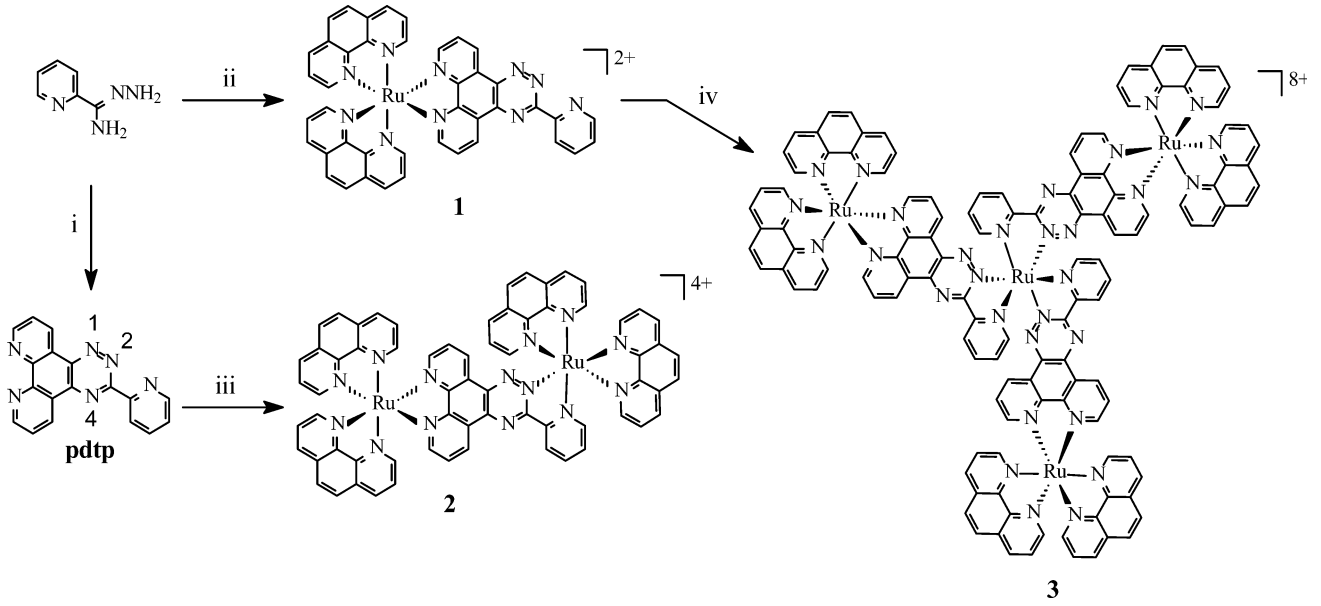

[a] (i) 1 equiv of phendione, (ii) $[(phen)_2Ru(phendione)]^{2+}$, (iii) $[Ru(bpy)_2Cl_2]$, (iv) $RuCl_3$.

symmetric bridging ligands. The study of polynuclear complexes, bridged with ligands composed of two nonequivalent chelating sites, has received a limited degree of attention.[16]

The ligand pdtp (pdtp = 3-(pyridin-2-yl)-as-triazino[5,6-f]1,10-phenanthroline) is a polyaromatic bridging ligand (Scheme 1).[17] It contains two nonequivalent chelating sites of which one is the nitrogen atoms of phenanthroline ring and the other is composed of one of the pyridyl ring and one of the 1,2,4-triazine ring. The precise electrochemical and photophysical properties of coordinated metal fragments will be site-specific due to the nonequivalence of the bridging ligand, and this may afford a route to modulate the directionality of electron (or energy) transfer between them. To our knowledge there is only one report related to its Ru(II) complexes, which merely described the synthesis and fluorescence properties of the mononuclear bis(phenanthroline)Ru(II) complex containing pdtp, and no other studies of this complex have been reported.[18]

In an attempt to obtain more insight into the interesting photochemical and photophysical properties of ruthenium complexes with asymmetric bridging ligands, we have synthesized and characterized the bridging ligand pdtp and corresponding ruthenium(II) complexes $[(phen)_2Ru(pdtp)]^{2+}$ (**1**) (phen = 1,10-phenanthroline), $[(phen)_2Ru(pdtp)Ru(phen)_2]^{4+}$ (**2**), and $[\{(phen)_2Ru(pdtp)\}_3Ru]^{8+}$ (**3**). The electrochemistry, absorption spectra, and luminescence properties (both at room temperature in fluid solution and at 80 K in rigid matrix) of complexes are also presented and discussed.

Experimental Section

Materials. 1,10-Phenanthroline-5,6-dione (phendione),[19] pyridine-2-carboxamide hydrazone,[20] *cis*-$[Ru(phen)_2Cl_2]\cdot 2H_2O$,[21] and $[Ru(phen)_2(phendione)](ClO_4)_2$[22] were prepared by the literature methods. Other reagents and solvents employed were commercially available and used as received without further purification.

Physical Measurements. Microanalysis (C, H, and N) was carried out with a Perkin-Elmer 240Q elemental analyzer. Absorption spectra were recorded on a Shimadzu UV-3101PC spectrometer. ^{1}H NMR spectra were recorded on Varian INOVA-500 spectrometer with $(CD_3)_2SO$ as solvent and $SiMe_4$ as an internal standard. Fast atomic bombardment mass spectra (FAB-MS) were obtained on a VG ZAB-HS spectrometer in a 3-nitrobenzyl alcohol matrix. Electrospray mass spectra (ES-MS) were measured on a LCQ system (Finnigan MAT, USA) using acetonitrile as mobile

(6) Haga, M.; Ali, M. M.; Koseki, S.; Fujimoto, K.; Yoshimura, A.; Nozaki, K.; Ohno, T.; Nakajima, K.; Stufkens, D. J. *Inorg. Chem.* **1996**, *35*, 3335.
(7) Wang, Y.; Perez, W. J.; Zheng, G. Y.; Rillema, D. P.; Huber, C. L. *Inorg. Chem.* **1998**, *37*, 2227.
(8) Hartshorn, C. M.; Daire, N.; Tondreau, V.; Loeb, B.; Meyer, T. J.; White, P. S. *Inorg. Chem.* **1999**, *38*, 3200.
(9) Baitalik, S.; Flörke, U.; Nag, K. *Inorg. Chem.* **1999**, *38*, 3296.
(10) Barthram, A. M.; Ward, M. D. *New J. Chem.* **2000**, *24*, 501.
(11) Pappenfus. T. M.; Mann, K. R. *Inorg. Chem.* **2001**, *40*, 6301.
(12) (a) Chao, H.; Ye, B. H.; Li, H.; Li, R. H.; Zhou, J. Y.; Ji, L. N. *Polyhedron* **2000**, *19*, 1975. (b) Chao, H.; Li, R. H.; Jiang, C. W.; Li, H.; Ji, L. N.; Li, X. Y. *J. Chem. Soc., Dalton Trans.* **2001**, 1920.
(13) (a) Di Pietro, C.; Serroni, S.; Campagna, S.; Gandolfi, M. T.; Ballardini, R.; Fanni, S.; Browne, W. R.; Vos, J. G. *Inorg. Chem.* **2002**, *41*, 2871. (b) Passaniti, P.; Browne, W. R.; Lynch, F. C.; Hughes, D.; Nieuwenhuyzen, M.; James, P.; Maestri, M.; Vos, J. G. *J. Chem. Soc., Dalton Trans.* **2002**, 1740.
(14) Börje, A.; Köthe, O.; Juris, A. *J. Chem. Soc., Dalton Trans.* **2002**, 843.
(15) Otsuki, J.; Omokawa, N.; Yoshiba, K.; Yoshikawa, I.; Akasaka, T.; Suenobu, T.; Takido, T.; Araki, K.; Fukuzumi, S. *Inorg. Chem.* **2003**, *42*, 3057.
(16) (a) Ward, M. D. *J. Chem. Soc., Dalton Trans.* **1993**, 1321. (b) Hage, R.; Lempers, E. B.; Haasnoot, J. G.; Reedijk, J.; Weldon, F. M.; Vos, J. G. *Inorg. Chem.* **1997**, *36*, 3139. (c) Fletcher, N. C.; Robinson, T. C.; Behrendt, A.; Jeffery, J. C.; Reeves, Z. R.; Ward, M. D. *J. Chem. Soc., Dalton Trans.* **1999**, 2999. (d) Gut, D.; Goldberg, I.; Kol, M. *Inorg. Chem.* **2003**, *42*, 3483. (e) Harriman, A.; Hissler, M.; Khatyr, A.; Ziessel, R. *Eur. J. Inorg. Chem.* **2003**, 955.
(17) Pabst, R. G.; Pfüller, O. C.; Sauer, J. *Tetrahedron Lett.* **1998**, *38*, 8825.
(18) Pabst, R. G.; Pfüller, O. C.; Sauer, J. *Tetrahedron* **1999**, *55*, 8045.
(19) Yamada, M.; Tanaka, Y.; Yoshimato, Y.; Kuroda, S.; Shimao, I. *Bull. Chem. Soc. Jpn.* **1992**, *65*, 1006.
(20) Case, F. H. *J. Heterocycl. Chem.* **1968**, *5*, 223.
(21) Sullivan, B. P.; Salmon, D. J.; Meyer, T. J. *Inorg. Chem.* **1978**, *17*, 3334.
(22) Goss, C. A.; Abruna, H. D. *Inorg. Chem.* **1985**, *24*, 4263.

phase. The spray voltage, tube lens offset, capillary voltage, and capillary temperature were set at 4.50 kV, 30.00 V, 23.00 V, and 200 °C, respectively, and the quoted *M*/*Z* values are for the major peaks in the isotope distribution.

Cyclic voltammetry was performed on an EG&G PAR 273 polarographic analyzer and 270 universal programmer. The supporting electrolyte was 0.1 M tetrabutylammonium perchlorate in acetonitrile freshly distilled from phosphorus pentaoxide and deaerated by purging with nitrogen. A standard three-electrode system was used comprising a platinum microcyclinder working electrode, platinum-wire auxiliary electrode, and a saturated calomel reference electrode (SCE).

For room temperature and 80 K emission spectra, each complex in a 4:1 (v/v) ethanol/methanol matrix was installed in the vacuum chamber with temperature controller. The samples were excited with frequency-double 400 nm Ti:sapphire laser with 250 fs pulse duration and 1 kHz repetition rate. The laser beam was focused on the samples with a spot size of 100 μm, and the exciting power is about 5 mW. The time-resolved emission spectra were measured using the streak camera (Hamamatsu, time resolution 25 ps). Acquisition of the streak images was performed via cooled CCD camera (Hamamatsu). Quantum yields of luminescence at room temperature were calculated according to literature procedures,[23] using an aerated aqueous solution of $[Ru(bpy)_3]^{2+}$ as reference emitter ($\phi = 0.028$[24]).

Molecular Orbital Calculations. The molecular structure of the free ligand pdtp was optimized by the INDO method[25] with the default parameters packaged in the computer program HyperChem Release 6 (HyperCube, Inc.).[26] Calculations of the electronic structures were carried out using the extended Hückel approximation[27] with the same program using the default parameters.

Synthesis. 3-(Pyridin-2-yl)-as-triazino[5,6-f]1,10-phenanthroline (pdtp). This ligand was prepared using the method similar to that as reference 17 with some modification. A mixture of pyridine-2-carboxamide hydrazone (0.20 g, 1.5 mmol) and phendione (0.32 g, 1.5 mmol) was refluxed with stirring in ethanol. In a few minutes, much yellow precipitate appeared. After 3 h of stirring, the insoluble material was removed by filtration while hot, washed with ethanol (3×5 cm^3), then dried at 50 °C in vacuo. Yield: 0.38 g, 82%. (Found: C, 65.92; H, 3.56; N, 25.73. Calcd for $C_{18}H_{10}N_6 \cdot H_2O$: C, 65.85; H, 3.66; N, 25.61%.) ^{1}H NMR (500 MHz, DMSO-d_6) δ 9.68 (d, 1H, $J = 8$), 9.63 (d, 1H, $J = 8$), 9.34 (d, 1H, $J = 8$), 9.30 (d, 1H, $J = 8$), 8.95 (d, 1H, $J = 3.5$), 8.81 (d, 1H, $J = 8$), 8.16 (t, 1H, $J = 7$), 8.03 (t, 1H, $J = 4.5$), 8.02 (t, 1H, $J = 4.5$), 7.70 (dd, 1H, $J_1 = 5$, $J_2 = 2.5$). FAB MS *m*/*z*: 311 ($C_{18}H_{10}N_6$ requires 310).

$[Ru(phen)_2(pdtp)](ClO_4)_2$ (1). The complex $[Ru(phen)_2(phendione)](ClO_4)_2$ (0.4 g, 0.46 mmol) was dissolved in acetonitrile (30 cm^3), and then pyridine-2-carboxamide hydrazone (0.075 g, 0.55 mmol) in ethanol (10 cm^3) was added dropwise. The mixture was refluxed for 5 h to give a red solution. After the solvent was removed by rotary evaporation, the crude product was collected and purified by column chromatography on alumina with acetonitrile−ethanol (15:1, v/v) as eluent. Yield: 0.32 g, 72%. (Found: C, 51.12; H, 2.68; N, 14.05. Calcd for $C_{42}H_{26}N_{10}Cl_2O_8Ru \cdot 2H_2O$: C, 50.09; H, 2.98; N, 13.92%.) ^{1}H NMR (500 MHz, DMSO-d_6): δ 9.87 (d, 1H, $J = 8$ Hz), 9.73 (d, 1H, $J = 8$ Hz), 8.99 (d, 1H, $J = 4.5$ Hz), 8.89 (d, 1H, $J = 8$ Hz), 8.81 (d, 2H, $J = 8$ Hz), 8.78 (d, 2H, $J = 8$ Hz), 8.40 (s, 4H), 8.32 (d, 2H, $J = 4$ Hz), 8.28−8.21 (m, 3H), 8.06 (d, 2H, $J = 6$ Hz), 7.99 (dd, 1H, $J_1 = 6$ Hz, $J_2 = 2$ Hz), 7.96 (dd, 1H, $J_1 = 6$ Hz, $J_2 = 2$ Hz), 7.81 (dd, 2H, $J_1 = 3$ Hz, $J_2 = 2$ Hz), 7.77 (t, 2H, $J = 4$ Hz), 7,75 (t, 1H, $J = 5$ Hz). ES MS (CH_3CN) *m*/*z*: 870.4 $[M - ClO_4]^+$, 386 $[M - 2ClO_4]^{2+}$.

$[(phen)_2Ru(pdtp)Ru(phen)_2](ClO_4)_4$ (2). A mixture of $[Ru(phen)_2Cl_2] \cdot 3H_2O$ (0.15 g, 0.27 mmol) and pdtp (0.042 g, 0.13 mmol) in ethanol−water (3:1 v/v, 60 cm^3) was refluxed for 8 h, during which time the solution turned deep red. After most of the ethanol was removed by rotatory evaporation, a deep red precipitate was obtained by dropwise addition of aqueous $NaClO_4$ solution. The product was puried by column chromatography on alumina with acetonitrile−ethanol (4:1 v/v) as eluent. Yield: 0.13 g, 63%. (Found: C, 48.18; H, 2.43; N, 11.95. Calcd for $C_{66}H_{42}N_{14}Cl_4O_{16}Ru_2 \cdot H_2O$: C, 48.05; H, 2.67; N, 11.89%.) ^{1}H NMR (500 MHz, DMSO-d_6): δ 9.89 (d, 1H, $J = 8.5$ Hz), 9.32 (d, 1H, $J = 8$ Hz), 8.92−8.82 (m), 8.79−8.73 (m), 8.67 (d, 1H, $J = 5.5$ Hz), 8.60 (d, 1H, $J = 5.5$ Hz), 8.47−8.36 (m), 8.33−8.16 (m), 8.08−7.89 (m), 7.87−7.68 (m). ES MS (CH_3CN) *m*/*z*: 1530 $[M - ClO_4]^+$, 715.7 $[M - 2ClO_4]^{2+}$, 444 $[M - 3ClO_4]^{3+}$, 309 $[M - 4ClO_4]^{4+}$.

$\{[(phen)_2Ru(pdtp)]_3Ru\}(ClO_4)_8$ (3). A suspension of $RuCl_3 \cdot 3H_2O$ (0.026 g, 0.1 mmol) in 20 cm^3 of glycerol was stirred at 100 °C under argon for 1.5 h. During this period, the color of the suspension changed to green. Then $[Ru(phen)_2(pdtp)](ClO_4)_2$ (0.29 g, 0.3 mmol) was added, and the solution temperature was maintained at 120 °C for 12 h. The solution was cooled to room temperature, and 60 cm^3 H_2O was added. After filtration, a dark red precipitate was obtained by dropwise addition of aqueous $NaClO_4$ solution. The product was purified by SP-Sephadex C-25 cation exchange chromatography with a solution 0.5 M NaCl in water/acetone (5:1) as eluent. Yield: 0.18 g, 55%. (Found: C, 46.35; H, 2.23; N, 12.96. Calcd for $C_{126}H_{78}N_{30}Cl_8O_{32}Ru \cdot 3H_2O$: C, 46.32; H, 2.39; N, 12.87%.) ^{1}H NMR (500 MHz, DMSO-d_6): δ 9.88 (m), 9.34 (m), 8.88−8.68 (m), 8.66−8.45 (m), 8.42−8.35 (m), 8.32−8.22 (m), 8.19−7.92 (m), 7.90−7.64 (m). ES MS (CH_3CN) *m*/*z*: 1506.0 $[M - 2ClO_4]^{2+}$, 970.8 $[M - 3ClO_4]^{3+}$, 703.1 $[M - 4ClO_4]^{4+}$, 542.8 $[M - 5ClO_4]^{5+}$.

CAUTION! Perchlorate salts of metal complexes with organic ligands are potentially explosive, and only small amounts of the material should be prepared and handled with great care.

Results and Discussion

Synthesis. An outline of the synthesis of the ligand and complexes is presented in Scheme 1. The ligand was synthesized on the basis of the method established by Case.[20] This method provides a very convenient way to prepare various compounds containing a 1,2,4-triazine ring. In this case, the condensation reaction time was reduced to 3 h and not found to lower the yield in comparison with the literature.[17] The ligand pdtp is an asymmetric ligand which can coordinate to metal ions via two different sites; one is the nitrogen atoms of phen ring, and the other is composed of one of the pyridyl ring and one of the 1,2,4-triazine ring. The dinuclear complex **2** was obtained from pdtp with 2 equiv of $[Ru(phen)_2Cl_2] \cdot 2H_2O$ in boiling ethanol−H_2O mixtures. Obviously, there can be two isomers involving N^2 and N^4 of the triazine ring. However, in this case it is obvious that the coordination is at N^2 rather than N^4 from the viewpoint of the steric hindrance between the ligands. Similar cases had been reported.[28,29] When the reaction between

(23) Demas, J. N.; Crosby, G. A. *J. Phys. Chem.* **1971**, *75*, 991.
(24) Nakamaru, K. *Bull. Chem. Soc. Jpn.* **1982**, *55*, 2697.
(25) Murrell, J. N.; Harget, A. J. *Semiempirical Self-consistent-field Molecular Orbital Theory of Molecules*; Wiley-Interscience: New York, 1971.
(26) *Hyperchem Release 6.01 for Windows*; Hypercube Inc., 2000.
(27) Hoffmann, R. *J. Chem. Phys.* **1963**, *39*, 1397.

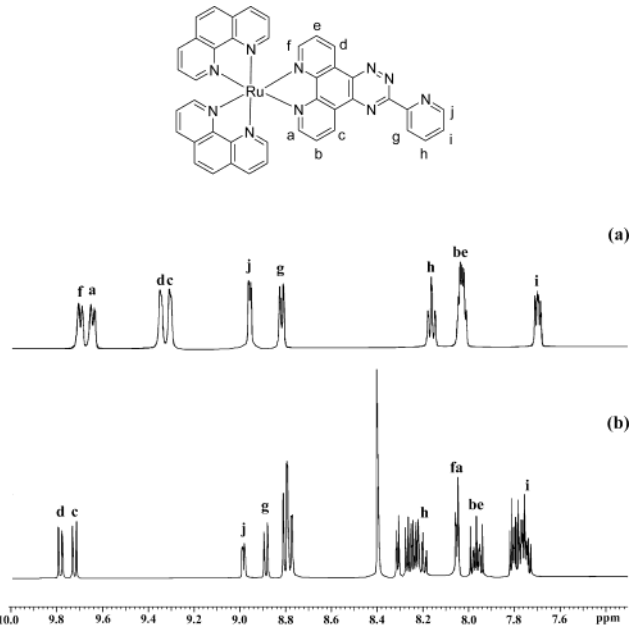

Figure 1. ^{1}H NMR spectra of pdtp (a) and $[Ru(phen)_2(pdtp)]^{2+}$ (b) in the aromatic region between δ 7.6 and 10.0 [DMSO-d_6 solvent, TMS reference].

$[Ru(phen)_2Cl_2]$ and pdtp was run in a 1:1 molar ratio in glycerol, the main product is the dinuclear complex **2**, and only very little mononuclear complex was obtained. Therefore, to prepare the aimed mononuclear complex **1**, we have carried out the condensation of pyridine-2-carboxamide hydrazone with the precoordinated phendione in $[Ru(phen)_2(phendione)]^{2+}$ to avoid the formation of the dinuclear complex and the other mononuclear complex coordinated by pyridine and triazine (Scheme 1). The reaction of $RuCl_3$ with 3 equiv of the mononuclear complex **1** in glycerol afforded the tetranuclear complex **3**. In our studies, we did not observe any oxidative degradation caused by the 1,2,4-triazine moiety at higher reaction temperature as reported before.[18] All these complexes were purified by column chromatography (mono- and dinuclear complexes on alumina, tetranuclear complex on SP Sephadex C-25) and characterized by elemental analysis, NMR, and ES MS.

^{1}H NMR Spectra. The ^{1}H NMR spectrum of free pdtp in DMSO-d_6 shows eight sets of signals in the aromatic region, as illustrated in Figure 1. The signal assignment is rather straightforward by the aid of ^{1}H$-^1$H COSY experiments and the comparison of chemical shifts with those of similar oligopyridines.[28−32] Unlike other symmetric phen derivatives, the chemical shifts of H_d, H_e, and H_f are observed to be downfield in comparison with those of H_a, H_b, and H_c, respectively. In pdtp ligand, the triazine ring is an electron-withdrawing group, and N^1 and N^2 are close to the H_d-H_f ring, so the electron-withdrawing effect of the triazine ring on the H_d-H_f ring is stronger than that of the H_a-H_c ring. Similar cases have been reported.[28]

Figure 1 also shows the ^{1}H chemical shift diagrams of mononuclear complex **1**. On coordination to one ruthenium ion, the protons on the phen ring all experience large shifts in comparison with those of free pdtp: H_c and H_d shows 0.42 and 0.45 ppm downfield shifts, H_b and H_e about 0.1 ppm upfield shifts, while H_a and H_f experience surprising upfield shifts of 1.62 and 1.58 ppm, respectively. The dramatic upfield shifts of H_a and H_f may be attributed to the effect of the ring current of the phen ligands. On the contrary, the chemical shifts of H_g, H_h, H_i, and H_j on the pyridine ring remain almost unchanged. This also indicates that the nitrogen atom of the pyridine ring does not coordinate.

It is interesting to note that in the ^{1}H NMR spectrum of dinuclear complex **2** the chemical shift of H_c remains almost unaltered upon coordination, in comparison with that of the pdtp ligand. This is different with that observed in the mononuclear complex above and due to the steric hindrance existing in the asymmetric bridging ligand. In complex **1**, the pyridine ring can be rotated to a suitable angle to relieve the steric interaction between it and the phen ring. However, in complex **2** the nitrogen atoms of the pyridine and triazine rings coordinate to Ru^{II}; therefore, the pyridine ring cannot rotate freely. The other resonance peaks are too complicated (two metal centers are bridged asymmetrically) to be assigned.[33] The more complicated behaviors are observed in the tetranuclear complex **3**. For $[\{(bpy)_2Ru(pdtp)\}_3Ru]^{8+}$, the central Ru^{II} with three asymmetric bridging ligands can exist as facial (*fac*) or as meridional (*mer*) isomers.[34] In the *fac* isomer, the three pdtp are magnetically equivalent (C_3 symmetry) giving rise to only one set of protons in the NMR spectrum. The *mer* isomer on the other hand possesses C_1 symmetry, with all three of the ligands inequivalent, which results in the presence of three different sets of proton in the NMR spectrum. Since for complex **3** only a mixture of *fac* and *mer* isomers was isolated, the NMR spectrum proved to be very complicated, as it contains signals for four sets of protons for pdtp, and many of them occupy very similar regions due to the similarity of the signals.

Mass Spectroscopy. The structures of mono-, di-, and tetranuclear complexes were further established by electrospray mass spectrometry (ESMS) in CH_3CN. This technique has proven to be very helpful for identifying polynuclear transition metal complexes with high molecular masses.[35] Usually, the mass is calculated from a series of multiply charged ions obtained by the successive loss of counteranions. In the ESMS spectra for the complexes, the mono- and dinuclear complexes exhibit all of the expected peaks due

(28) Hage, R.; Van Diemen, J. H.; Ehrlich, G.; Haasnoot, J. G.; Stufkens, D. J.; Snoeck, T. L.; Vos, J. G.; Reedijk, J. *Inorg. Chem.* **1990**, *29*, 988.
(29) Chao, H.; Yang, G.; Xue, G. Q.; Li, H.; Zhang, H.; Williams, I. D.; Ji, L. N.; Chen, X. M.; Li, X. Y. *J. Chem. Soc., Dalton Trans.* **2001**, 1326.
(30) Jahng, Y.; Thummel, R. P.; Bott, S. G. *Inorg. Chem.* **1997**, *36*, 3133.
(31) Ye, B. H.; Chen, X. M.; Zeng, T. X.; Ji, L. N. *Inorg. Chim. Acta* **1995**, *240*, 5.
(32) Nair, R. B.; Teng, E. S.; Kirkland, S. L.; Murphy, C. J. *Inorg. Chem.* **1998**, *37*, 139.
(33) Chirayil, S.; Hegde, V.; Jahng, Y.; Thummel, R. P. *Inorg. Chem.* **1991**, *30*, 2821.
(34) (a) Hage, R.; Haasnoot, J. G.; Reedijk, J.; Vos. J. G. *Inorg. Chim. Acta* **1986**, *118*, 73. (b) Fletcher, N. C.; Nieuwenhuyzen, M.; Rainey, S. *J. Chem. Soc., Dalton Trans.* **2001**, 2641.
(35) (a) Arakawa, R.; Tachiyashiki, S.; Matsuo, T. *Anal. Chem.* **1995**, *67*, 4133. (b) Moucheron, C.; Kirsch-De Mesmaeker, A. *J. Am. Chem. Soc.* **1996**, *118*, 12834.

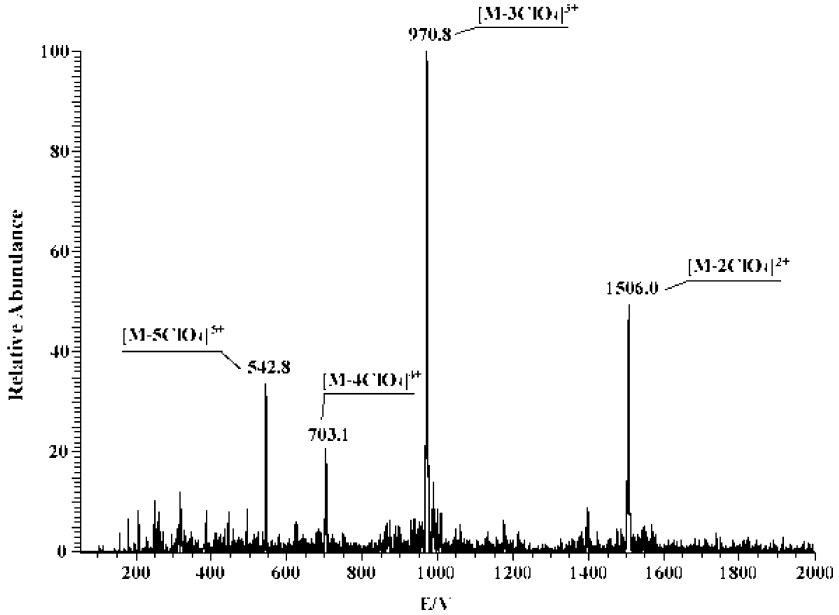

Figure 2. The ESMS spectrum of $[\{(phen)_2Ru(pdtp)\}_3Ru]^{8+}$.

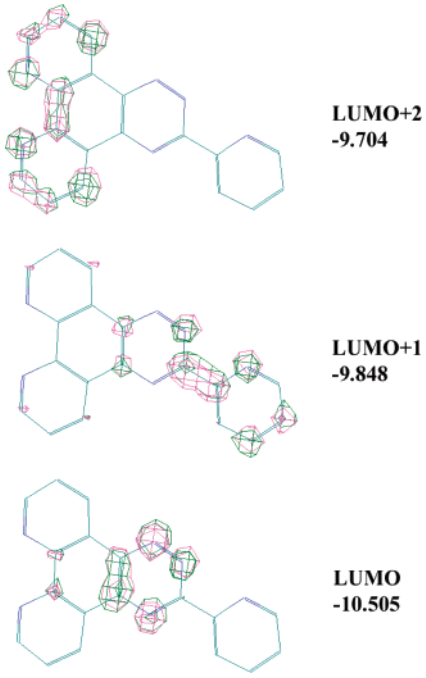

Figure 3. Graphical illustrations for the three lowest lying unoccupied orbitals of pdtp.

to $[M - nClO_4]^{n+}$ cations; however, for the tetranuclear complex **3**, only the charge state distribution ranging from 5+ to 2+ can be clearly observed (Figure 2). The measured molecular weights were consistent with expected values.

Molecular Orbital Calculations. Extended Hückel calculations were carried out in order to obtain compositions and energies of the pdtp ligand orbitals and to rationalize the electrochemical and spectroscopic results. Figure 3 shows the graphical illustrations of the squared MO coefficients for the three lowest lying unoccupied orbitals of pdtp. For this ligand, we made the following observations: (i) the lowest vacant molecular orbital is centered on the triazine part with the electronic distribution. The LUMO is found at −10.505 eV, and this orbital is at significantly lower energy than the LUMO in isolated phen (−9.714 eV). (ii) The next vacant MO LUMO + 1 lying at higher energy (−9.848 eV) is extended on the pyridine-type part with a strong weight on the related coordinating nitrogens and no more electronic density on the phen-type nitrogens. (iii) In contrast, the MO LUMO + 2 (−9.704 eV) is developed on the phenanthroline-type part and with very little electronic density on the pyridine-type nitrogen and the triazine part. This simple electronic approach reflects the nonequivalent nature of two coordinating sites on the asymmetric bridging ligand pdtp. This electronic distribution and the orbital energy levels account also for the more pronounced π-attractor character and the greater energetic stabilization of the radical anion of pdtp with respect to those of the phen ligand.

Table 1. Redox Potentials for the Ruthenium(II) Complexes[a]

complex	$E_{1/2}^{ox}$		$E_{1/2}^{red}$				
$[Ru(phen)_3]^{2+}$ [b]	+1.27		−1.35	−1.52			
1	+1.39		−0.84	−1.35	−1.58		
2	+1.41	+1.56	−0.42	−1.34	−1.53		
3	+1.43		−0.45	−0.59	−0.78	−1.37	−1.56

[a] All complexes were measured in 0.1 M NBu_4ClO_4−CH_3CN, error in potentials ±0.02 V; $T = 23 \pm 1$ °C; scan rate = 100 mV S^{-1}. [b] Data from ref 36.

Electrochemistry. The electrochemical behaviors of complexes **1**−**3** have been studied in CH_3CN by cyclic voltammetry, and the data are summarized in Table 1. The cyclic voltammograms of **2** and **3** are illustrated in Figure 4. All of these complexes exhibit a number of ligand-based redox couples in the potential range 0 to −2.0 V (vs SCE); these results can further be rationalized with the molecular orbital calculation results. As seen in Figure 3, the LUMO is mainly centered on the triazine portion of pdtp; it is 0.791 eV lower in energy than the LUMO orbital of phen, so the first reduction of complex **1** is assigned to the bridge pdtp. While the LUMO + 1 of pdtp is also lower in energy than the LUMO orbital of phen, the presence of one additional

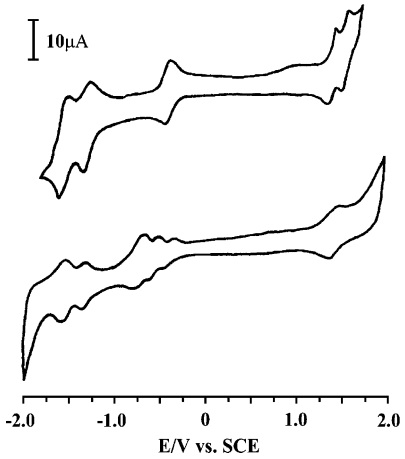

Figure 4. Cyclic voltammogram of complexes **2** (top) and **3** (bottom) in acetonitrile at room temperature.

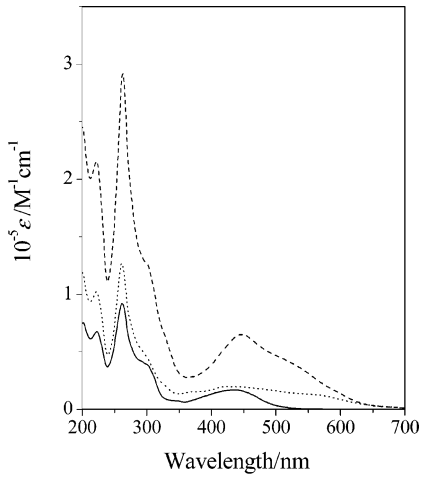

Figure 5. Absorption spectra of complexes **1** (—), **2** (- - -), and **3** (···) in CH_3CN at room temperature.

electron on the triazine site of pdtp is expected to raise its energy, so the second and third reductions should involve the phen ligands. For di- and tetranuclear complexes, introduction of other Ru^{II} moieties at the remote bidentate site of $[Ru(phen)_2(pdtp)]^{2+}$ results in a positive shift in the reduction potential of the pdtp ligand, reflecting a net stabilization of the π^* orbital of the bridging relative to the terminal ligand. The cyclic voltammogram of complex **3** shows a set of three reversible reduction waves assigned to the three $pdtp^{0/-1}$ processes. The separation between successive waves with the set of $pdtp^{0/-1}$ reductions increases from 0.16 to 0.19 V, consistent with the overall charge reduction.

The mononuclear complex **1** exhibits one reversible oxidation at +1.39 V, which is more positive than that of $[Ru(phen)_3]^{2+}$.[36] This also suggests that the better π^* acceptor character of pdtp ligand stabilizes the ruthenium-based HOMO, rendering the oxidation of the metal more difficult. In the dinuclear complex **2** two closely spaced oxidation waves at +1.41 and +1.56 V are observed. The difference (150 mV) of the redox potentials may be attributed to the nonequivalence of the two coordination sites of the bridging ligand and/or the metal−metal interaction between the two metal centers, as observed in other asymmetric dinuclear complex $[(bpy)_2Ru(AB)Ru(bpy)_2]^{2+}$ (AB = 2,2′:3′,2″:6″,2‴-quaterpyridine)[36] and $[(dmb)_2Ru(\mu\text{-eilatin})Ru(dmb)_2]^{4+}$ (dmb = 4,4′-dimethyl-2,2′-bipydine).[16d] The metal−metal interaction via the bridging ligand pdtp may be explained on the basis of superexchange theory,[1c] where the electronic coupling between metal orbitals is mediated through those of the bridging ligand. However, as shown in molecular orbital calculations, there is a little communication between two chelating sites of pdtp. This means that the metal−metal interaction in dinuclear complex **2** is fairly weak. So the rise in potentials of complex **2** may be mainly ascribed to the different coordination environments of two metal centers.

In the tetranuclear complex **3**, the central Ru ion is surrounded by three pdtp; it is a different coordination environment from the three peripheral subunits (Scheme 1). Because pdtp is a better electron withdrawing ligand than phen, oxidation of the central metal is expected to occur at more positive potential than that of the three peripheral metals. It has been reported that the central metal ion of tetranuclear complexes with a π-accepting tpphz bridging ligand oxidized at 0.1−0.15 V higher potential compared to that of peripheral subunits.[5b] However, in cyclic voltammograms of **3** only one three-electron oxidation wave (+1.43 V) was observed, which by comparison with the oxidation peaks of the corresponding mononuclear complex is attributed to simultaneous one-electron oxidations of the three noninteracting peripheral ruthenium centers. This situation is similar to that found in acetonitrile for other tetranuclear Ru^{II} complexes based on the 2,3-bis(2′-pyridyl)pyrazine (dpp) bridging ligand,[2a] but in that case, the disappearance of the oxidation for the central Ru^{II} was due to the strong interaction between the peripheral and the central Ru^{II} and the oxidation of the inner Ru^{II} was displaced out of the potential window available. In the present system, the reason for such a behavior is the nonequivalent coordination environments. As observed in dinuclear complex, the difference of two oxidation waves is quite distinct. In the tetranuclear complex, this difference will be further enlarged with two $[(phen)_2Ru(pdtp)]^{2+}$ instead of phen. Therefore, the oxidation potential of the central metal in complex **3** cannot be seen within the potential window examined.

Absorption Spectra. The absorption spectra of the complexes are shown in Figure 5, and the energy maxima and absorption coefficients are summarized in Table 2. The spectrum of complex **1** consists of three well-resolved bands at 435, 263, and 223 nm in the range 200−700 nm. The bands at 263 and 223 nm are attributed to the $\pi-\pi^*$ intraligand transitions by comparison with the spectrum of $[Ru(phen)_3]^{2+}$.[38,39] The lowest energy band at 435 nm is

(36) Barigelletti, F.; Juris, A.; Balzani, A.; Belser, P.; Von Zelewsky, A. *Inorg. Chem.* **1987**, *26*, 4115.

(37) Bardwell, D. A.; Barigelletti, F.; Cleary, R. L.; Flamigni, L.; Guardigli, M.; Jeffery, J. C.; Ward, M. D. *Inorg. Chem.* **1995**, *34*, 2438.

(38) Kawanishi, Y.; Kitamura, N.; Kim, Y.; Tazuke, S. *Riken Q.* **1984**, *78*, 212.

(39) Cocks, A. T.; Wright, R. D.; Seddon, K. R. *Chem. Phys. Lett.* **1982**, *85*, 369.

Table 2. Spectroscopic and Photophysical Data

complex	absorption (MLCT)[a] 298 K λ_{max}, nm (ϵ, M^{-1} cm^{-1})	emission[b] 298 K λ_{max}, nm	τ, ns	ϕ_{em}	80 K λ_{max}, nm	τ, μs
$[Ru(phen)_3]^{2+}$ [c]	442 (18000)	604	460	2.8×10^{-2}	565	10.00
1	434 (17000)	612	464	9.1×10^{-3}	581 616	4.77
2	551[e] (13000), 434 (19700)	612	142	2.3×10^{-4}	566 613	8.84
3[d]	552[e] (30200), 447 (65000)				676	4.16

[a] Solvent, acetonitrile. [b] Matrix, EtOH/MeOH 4:1. [c] Data from refs 38 and 39. [d] The lifetime of complex **3** was not measured because of the poor resolution of the emission band. [e] Data from the mathematical deconvolution of the spectra.

assigned to metal−ligand charge transfer (MLCT). For mixed-ligand complexes, the interpretation becomes more complex, since there are multiple $d\pi-\pi_1^*$ and $d\pi-\pi_2^*$ transitions. The Ru($d\pi$) → pdtp(π^*) and Ru($d\pi$) → phen(π^*) transitions cannot be separated from one another as observed for other mixed-ligand diimine complexes.[40−42] This band is blue shifted in comparison with that of $[Ru(phen)_3]^{2+}$, which can be attributed to the increased π-delocalization and thus π-acceptor capacity of the pztp ligand, resulting in decreased electron density on the Ru and in turn stabilization of the metal d_π orbital.

Going from the mononuclear complex **1** to the dinuclear complex **2**, a broad MLCT band with shoulder peak is exhibited in the spectra, and no significant red shift of the band maximum occurs. A similar behavior is also observed for the tetranuclear complex **3**. This is sharp contrast to π-accepting bridging systems such as bbdb [1,4-bis(4′-methyl-2,2′-bipyridin-4-yl)buta-1,3-diene],[43] and dpp [2,3-bis(2-pyridyl)pyrazine].[2a] Generally, the addition of a second metal ion at the remote coordination site of the bridging ligand results in stabilization of the π^* level of the bridging ligand, leading to enhanced $d\pi \rightarrow \pi^*$ orbital overlap. This effect lowers the HOMO−LUMO gap, which results in a low-energy shift of the MLCT bands in the dinuclear complexes. However, in our case, the asymmetry of the complex decreases the overlap of the Ru($d\pi$) → pdtp(π^*) transitions and broadens the MLCT band.

It is now well established that the lowest energy MLCT transitions are linearly related to the difference between the potential for the first one-electron oxidation (HOMO) and the first one-electron reduction (LUMO) ($\Delta E_{1/2}$).[7,36,44] Electrochemical data were used to calculate the expected energy transitions for the MLCT bands and are listed in Table 3. As a result, the lowest energy MLCT transitions are all expected to be Ru($d\pi$) → pdtp(π^*) and occur in the near-IR region of the spectra, but experimentally, absorptions in this region were small or even not observed. Within the pdtp series of complexes, the MLCT bands involving the Ru-bound phenanthroline-like portion of pdtp more closely match the Ru($d\pi$) → phen(π^*) transitions, e.g., 442 nm for $[Ru(phen)_3]^{2+}$. This is similar to that observed in $[Ru(bpy)_2(dppz)]^{2+}$,[45] for which the redox and optical orbitals are different in nature. As discussed before, the metal−metal interaction in the dinuclear complex is fairly weak; the difference induced is mainly ascribed to the nonequivalent coordination environments. If we think of the two Ru units in dinuclear complex as independent moieties, and the two oxidations (+1.41 and +1.56 V vs SCE) observed are attributed to the first one-electron oxidation of them, respectively, we can find that the MLCT bands involving the Ru-bound pyridyltriazine-like portion of pdtp are exhibited in the near-IR region and assigned to the Ru($d\pi$) → pdtp(π^*) transitions as expected. This indicates that in dinuclear and tetranuclear complexes the MLCT bands are a mixture of two remarkably different transitions, and each retains its identity and scales up in intensity with the number of the metal centers and ligands. The reason for this is not known at present, but it is consistent with broadening of the MLCT band instead of the normally observed red shift on passing from mononuclear to dinuclear and tetranuclear complexes.

Luminescence Properties. The emission spectra of complexes are recorded in 4:1 EtOH/MeOH at room temperature (Figure 6) or 80 K (Figure 7). The emission of tetranuclear complex **3** is too weak to measure at room temperature. Emission decays of all complexes are monoexponential. The emission band maxima, excited-state lifetime (τ), and emission quantum yields (ϕ_{em}) obtained are collected in Table 2.

Emission of Ru(II) polypyridine complexes usually occurs from the lowest-lying ^{3}MLCT excited state.[46−48] This assignment holds true for our complexes. The blue-shift and appearance of vibrational structure on lowering the temperature are typical of MLCT Ru-based emitters and are mainly due to the impossibility for the frozen solvent to reorganize around the excited molecule. The longer luminescence lifetimes at 80 K with respect to those at room temperature can be attributed to slowing down of the radiationless transitions on decreasing temperature.

The mono- and dinuclear complexes in EtOH/MeOH all emit at the same wavelength (612 nm). It is interesting to observe that the emission intensity of mononuclear complex **1** is much stronger than that of dinuclear complex **2** at room temperature (Figure 6). At the same time, the excited-state lifetime (τ) at room temperature for **1** is larger than that observed for **2** (Table 2). This can be attributed to an enhanced rate constant of the radiationless transitions due to the energy gap law[47,48] and modification in the nature of

(40) Braunstein, C. H.; Baker, A. D.; Strekas, T. C.; Gafney, H. D. *Inorg. Chem.* **1984**, *23*, 857.
(41) Sahai, R.; Morgan, L.; Rillema, D. P. *Inorg. Chem.* **1988**, *27*, 2495.
(42) Show, J. R.; Webb, R. T.; Scheml, R. H. *J. Am. Chem. Soc.* **1990**, *112*, 1117.
(43) Baba, A. I.; Ensleg, H. E.; Schmehl, R. H. *Inorg. Chem.* **1995**, *34*, 1198.
(44) Boyde, S.; Strouse, G. F.; Jones, W. E., Jr.; Meyer, T. J. *J. Am. Chem. Soc.* **1990**, *112*, 7395.
(45) Amouyal, E.; Homsi, A.; Chambron, J.-C.; Sauvage, J.-P. *J. Chem. Soc., Dalton Trans.* **1990**, 1841.
(46) Belser, P.; Von Zelewsky, A.; Juris, A.; Barigelletti, F.; Balzani, V. *Gazz. Chim. Ital.* **1983**, *113*, 731.
(47) Meyer, T. J. *Pure Appl. Chem.* **1986**, *58*, 1193.
(48) Juris, A.; Balzani, V.; Barigelletti, F.; Campagna, S.; Belser, P.; Von Zelewsky, A. *Coord. Chem. Rev.* **1988**, *84*, 85.

Table 3. Predicted UV−Vis Absorption Maxima Based on Electrochemistry Data

	$E_{1/2}$, V										
	oxidation		reduction		$\Delta E_{1/2}(1)^a$	$\lambda_1(\max)^b$	$\Delta E_{1/2}(2)^c$	$\lambda_2(\max)^d$	$\Delta E_{1/2}(3)^e$	$\lambda_3(\max)^f$	$\lambda_4(\max)^g$
complex	oxidation 1	oxidation 2	pdtp	phen	V	nm	V	nm	V	nm	nm
1	+1.40		−0.84	−1.35	2.24	553			2.75	451	434
2	+1.41	+1.56	−0.42	−1.34	1.83	677	1.98	626	2.75	451	434
3	+1.43		−0.45	−1.37	1.88	659			2.80	443	447
$[Ru(phen)_2]^{2+}$	+1.27			−1.35					2.62	473	442

[a] $\Delta E_{1/2}(1) = E_{1/2}$(oxidation 1) − $E_{1/2}$(first pdtp reduction). [b] λ_1(max) was calculated on the basis of $\Delta E_{1/2}(1)$ data. [c] $\Delta E_{1/2}(2) = E_{1/2}$(oxidation 2) − $E_{1/2}$(first pdtp reduction). [d] λ_2(max) was calculated on the basis of $\Delta E_{1/2}(2)$ data. [e] $\Delta E_{1/2}(3) = E_{1/2}$(oxidation 1) − $E_{1/2}$(first phen reduction). [f] λ_3(max) was calculated on the basis of $\Delta E_{1/2}(3)$ data. [g] The experimental data.

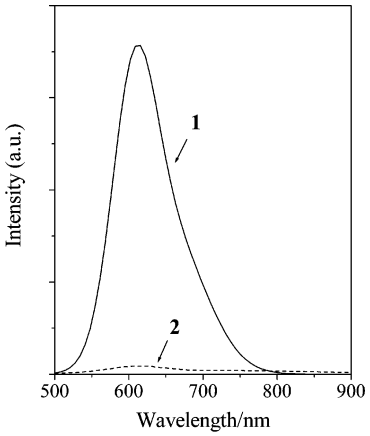

Figure 6. Emission spectra of complexes **1** (—) and **2** (- - -) in EtOH/MeOH 4:1 (v/v) at room temperature.

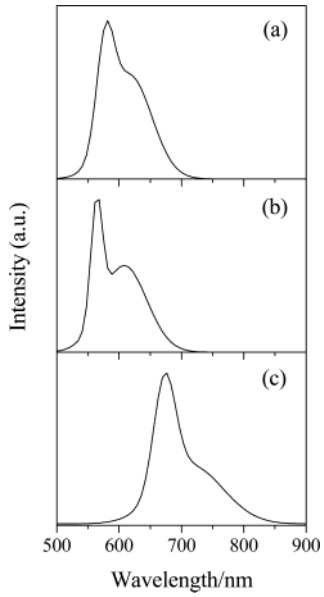

Figure 7. Emission spectra of complexes **1** (a), **2** (b), and **3** (c) in EtOH/MeOH 4:1 (v/v) rigid matrix at 80 K.

the excited state. It has been reported that the emissions from some Ru(II) pyridyltriazine complexes at room temperature are very weak.[28] However, it is also noted that at 80 K the dinuclear complex **2** possesses a longer lifetime (8.84 μs) in comparison with that of mononuclear complex **1** (4.77 μs). This is a quite different behavior from that observed at room temperature, indicating that the excited state of **2**, but not that of **1**, undergoes a thermally driven fast radiationless transition at room temperature.

In supramolecular antenna systems, migration of the excitation energy between central and peripheral units is normally assumed to proceed via intercomponent energy transfer processes. As pointed out before, complexes studied here contain two transitions at different energy levels due to the nonequivalence of the bridging ligand. One involves the phenanthroline moiety ($Ru_1\rightarrow$ pdtp), and the other one involves the pyridyltriazine moiety ($Ru_2\rightarrow$ pdtp). In tetranuclear complex **3**, the latter does not directly contribute to the emission process, and energy transfer from $Ru_2\rightarrow$ pdtp CT excited state to $Ru_1\rightarrow$ pdtp CT takes place. This process is especially obvious at 80 K where the emission band shifts toward lower energies compared to the emission of dinuclear complex **2** and suggests that the luminescent levels involve the peripheral metals rather than the central chromophore.

Conclusion

A series of mono-, di-, and tetranuclear Ru(II) complexes with an asymmetric bridging ligand pdtp have been synthesized and characterized. Molecular orbital calculation reflects the nonequivalent nature of two coordinating sites on the asymmetric bridging ligand pdtp. This is further testified in the electrochemical studies and absorption spectra. Electrochemical data show that the first redox process in these complexes is pdtp based and the metal−metal interaction in di- and tetranuclear complexes is very weak. Absorption spectra are essentially the sum of the spectra of the component monometallic species. All of the complexes exhibit emission originating from the lowest energy MLCT excited state and are close to that featured by the parent $[Ru(phen)_3]^{2+}$ species. It is also interesting to observe that the nonequivalent bridging ligand directs center-to-periphery energy transfer occurring in the dendritic tetranuclear complex.

Acknowledgment. We are grateful to the NNSF of China, the RGC of Hong Kong, the NSF of Guangdong Province, the Hong Kong University of Science and Technology, and the Research Fund of Royal Society of Chemistry U.K. for their financial support.

Supporting Information Available: Figures S1−S3 showing emission decays of complexes **1**−**3** in EtOH/MeOH 4:1 (v/v) rigid matrix at 80 K. This material is available free of charge via the Internet at http://pubs.acs.org.

IC034769Z